Investigation of Microwave Attenuation Measurements in a Laboratory-Scale Rocket Motor Plume

Robert A. Frederick Jr.,* John A. Blevins,†
and
Hugh W. Coleman‡
University of Alabama in Huntsville, Huntsville, Alabama 35899

Introduction

Overview

THE use of microwave diagnostics in rocket exhaust studies can allow determination of electron density and provide information concerning communication signal reception and radar signature. The classical presentation of microwave measurement techniques is for use in underdense or low-collision plasmas,[1,2] such as rocket exhausts at low back pressures.[3] In contrast, this investigation is concerned with electron density determinations in rockets exhausting at atmospheric pressure. The appropriate use of assumptions is reviewed, and a graphical presentation of index-of-attenuation behavior is provided to supplement the assessment of the experimental results.

An experimental investigation using multiple-frequency microwave diagnostics was performed to assess the use of microwave attenuation measurements in laboratory-scale solid-rocket exhaust plumes for ranking propellants according to their production of electrons. The challenges of this work are interpreting measurements in a collisional plasma coupled with the small plume diameter of the laboratory-scale rocket exhaust.

Rocket Exhaust Plume Diameter

The rocket plume diameter considered in microwave experimental studies is the diameter of the region of highly ionized gases, since it is the ionization mechanisms that affect the wave propagation properties. Balwanz[3] reported that at atmospheric pressure, experimental studies have shown that the visible flame boundaries do represent ionization boundaries from afterburning effects. This is true because the mean free path at atmospheric pressure is sufficiently small that the electrons collide with molecules and lose their energy at very short distances from the visible flame boundary. Therefore, for studies at atmospheric pressures, such as this investigation, photographic or video methods are valid for estimating the plume diameter.

Experimental Approach

A test matrix of 15 laboratory-scale rocket motor firings was conducted at the U.S. Army Missile Command's solid-rocket test site, utilizing laboratory-scale solid rocket motors exhausting at atmospheric pressure. Dual-frequency microwave diagnostics were employed (17 and 35 GHz), and three propellants of different ionization potentials were evaluated to check the sensitivity of the microwave system. The goal of the experimental investigation was to assess the usefulness of microwave measurement techniques and, particularly, if microwave methods could be used on laboratory-scale rocket motors to rank propellants according to their propensity to produce electrons.

Received Feb. 24, 1994; revision received Feb. 24, 1995; accepted for publication March 2, 1995.

*Assistant Professor, Propulsion Research Center, Department of Mechanical and Aerospace Engineering. Senior Member AIAA.

†Graduate Research Assistant, Propulsion Research Center, Department of Mechanical and Aerospace Engineering. Student Member AIAA.

‡Eminent Scholar in Propulsion and Professor, Propulsion Research Center, Department of Mechanical and Aerospace Engineering. Senior Member AIAA.

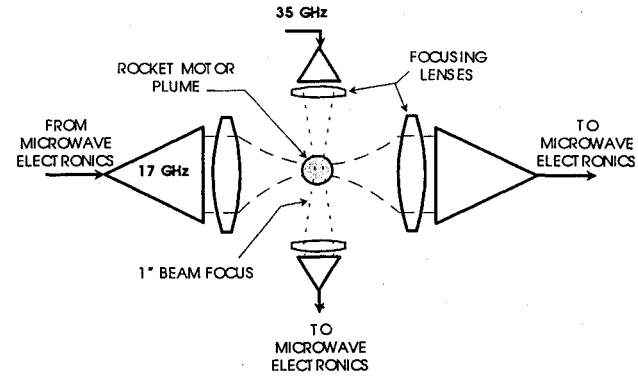

Fig. 1 Experimental setup.

The laboratory-scale rocket motors used in this experimental program were center-perforated solid rocket motors each having a 2-in.-o.d. propellant sleeve. The nozzle exit diameter for all rocket motors was 1 in., and the nozzle throat diameter was selected for each motor to obtain a combustion pressure of approximately 1500 psi.

The microwave diagnostic system is shown in Fig. 1. Dielectric focusing lenses were used to narrow the beam to a focus diameter of approximately 1 in. for both frequencies. The beam focus is one of the limiting factors when using microwave diagnostics in a laboratory-scale rocket motor. The smallest beam focus obtainable using any specific frequency is equal to the wavelength.

The propellants evaluated in the experimental program included an ammonium perchlorate (AP) with hydroxyl-terminated polybutadiene (HTPB), an AP/HTPB propellant with 2.34% potassium perchlorate as an additive to enhance ionization, and a high-energy nitramine-based propellant. The values of electrical properties of the propellants can be bounded by the frozen-flow and equilibrium-flow solutions, which can be determined by the NASA SP273 code.[4]

Discussion of Experimental Results

Representative results from the tests performed are shown in Fig. 2. The three attenuation profiles represent one test from each of the three propellants in the same rocket motor, axial measurement location, and microwave frequency. Therefore, an evaluation of the difference in test results should provide qualitative insight into the ranking of propellants according to their propensity to produce electrons (the overall goal of the experiments). From the given experimental results, it is evident that the microwave attenuation is greater in the nitramine-based propellant than in the AP with additives, which in turn has a higher attenuation than the AP without additives. Consequently, it can be concluded that the electron density of the nitramine-based propellant is greater than that of the AP with additives, which in turn has a greater electron density than the AP without additives. However, it should be noted that in the laboratory-scale rockets tested the attenuation values were so small for all the propellants that the magnitudes of the electron density are impossible to determine with any reasonable accuracy.

The data reduction for evaluation of electron density from the transmission attenuation measurements is accomplished through a series of equations. First, the index of attenuation χ is related to the transmission attenuation measurement as

$$T\,[\mathrm{dB}] = 20 \log_{10} \exp\left(\frac{\omega \chi}{c} d_p\right) \tag{1}$$

where T[dB] is the transmission attenuation in decibels, ω is the interrogation wave frequency, c is the speed of light, and d_p is the exhaust plume diameter. The plume diameter was estimated by evaluating the video record of each rocket motor firing. Second, the plasma frequency ω_p is related to the index of attenuation as

$$\chi = \left\{ \frac{1}{2}\left(1 - \frac{\omega_p^2}{\nu^2 + \omega^2}\right) + \frac{1}{2}\left[\left(1 - \frac{\omega_p^2}{\nu^2 + \omega^2}\right)^2 + \left(\frac{\omega_p^2}{\nu^2 + \omega^2}\left(\frac{\nu}{\omega}\right)\right)^2\right]^{\frac{1}{2}}\right\}^{\frac{1}{2}} \tag{2}$$

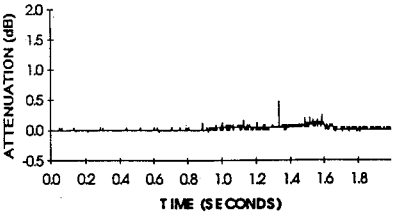

a) Ammonium perchlorate

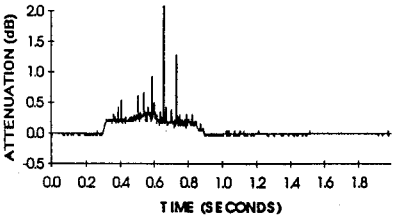

b) Ammonium perchlorate with additives

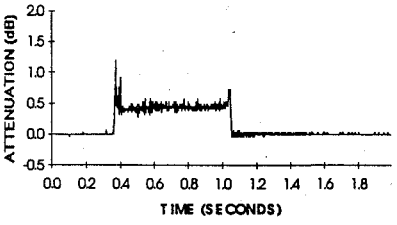

c) Nitramine with additives

Fig. 2 Experimental results.

where ν is the electron collision frequency. Lastly, the electron density n_e is related to the plasma frequency through

$$\omega_p = \left(\frac{n_e e^2}{\varepsilon_0 m_e}\right)^{\frac{1}{2}} \tag{3}$$

where e is the electron charge, ε_0 is the permittivity of free space, and m_e is the mass of an electron.

When using Eqs. (1–3) to evaluate the electron density from a single frequency measurement, the electron collision frequency ν must be known or estimated. If two frequencies are used, the equations for the index of attenuation, χ, can be set up as two equations with two unknowns (the plasma frequency ω_p and the electron collision frequency ν).

A consideration in calculating the electrical properties from low-attenuation measurements is the uncertainty in the calculated results. A jitter program[5] can be used to aid in estimating the uncertainty in the calculated results. In this study, a jitter program was used to determine that the electron collision frequency was very sensitive to small changes in attenuation and that assuming the full range of anticipated measurement uncertainty produced unreasonable solution pairs of electron collision frequency and electron density. Therefore, in this analysis it was chosen to bound the electron collision frequency by analytical estimates.

The measurement values and the results from using Eqs. (1–3) to iterate to a solution for the electron density for one of the nitramine tests are shown in Table 1. The uncertainty interval for n_e shown in Table 1 was determined by limiting the electron collision frequency ν to fall within the range of the analytical predictions. The electron density was then calculated for the range of attenuation uncertainty and predicted electron collision frequency values (1×10^{11}–1×10^{13}). The other tests using the nitramine propellant produced similar attenuation values.

Phase-shift measurements were also taken which confirmed the analytical assessment[6] that it is impossible to distinguish between different levels of electron density with phase-shift measurements in a collisional plasma.

The electron collision frequency for the nitramine-based propellant will be similar to that for the other propellants tested under the same atmospheric pressure. Therefore, using the nominally determined value for the electron collision frequency reported in Table 1,

Table 1 Uncertainty behavior of electrical properties in nitramine propellant tests

Parameter	Nominal value	Uncertainty interval
T[dB] 17 GHz	0.45	±0.05
T[dB] 35 GHz	0.42	±0.05
Electron collision frequency ν, collisions/s	7.1×10^{11}	$1 \times 10^{11} < \nu < 1 \times 10^{13}$
Electron density n_e, e/cm^3	2.8×10^{10}	$7.4 \times 10^{9} < n_e < 4.0 \times 10^{11}$

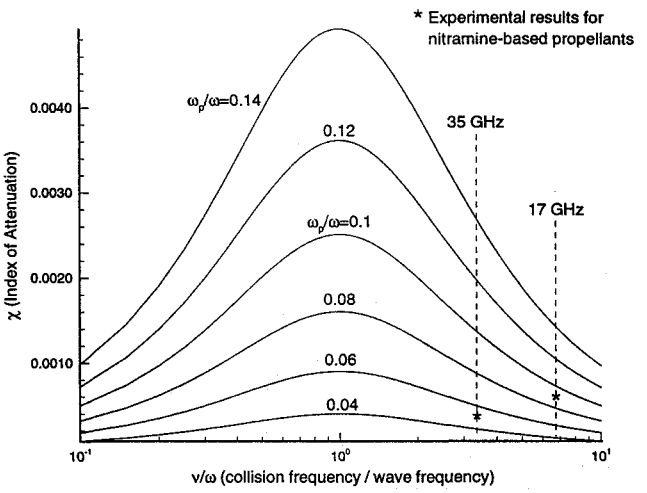

Fig. 3 Sensitivity of experimental setup.

the predicted measurement system response can be assessed by using Eq. (2). This can be best seen by graphically presenting χ from Eq. (2) vs ν/ω for lines of constant ω_p/ω (constant electron density) as presented in Fig. 3. The ability to discriminate between different levels of electron density using different microwave interrogation frequencies can be observed in this figure. For a known electron collision frequency and fixed interrogation wave frequency, the microwave diagnostic system can be associated with a fixed value of ν/ω. Based on the nominal values presented in Table 1, ν/ω is 6.6 for the 17-GHz interrogation wave frequency and 3.2 for the 35-GHz interrogation wave frequency. From this figure, it can be seen that the ability to distinguish between different levels of electron density may be achieved with attenuation measurements provided that the electron density values are high enough to be detected. Also, the 35-GHz interrogation wave frequency should provide greater resolution (accuracy) between different levels of electron density than the 17-GHz if the electron density is sufficiently high. Furthermore, this graph illustrates that, in contrast to conventional logic, an increase in the interrogation wave frequency does not always correspond to a decrease in attenuation. These trends for rocket exhausts at atmospheric pressure are also significant for communication signal transmission and optimizing the radar signature. The values of ω_p/ω for the nitramine-based propellant corresponding to the nominal values presented in Table 1 are also plotted in Fig. 3.

Conclusions

For rockets exhausting at atmospheric pressure, as in this investigation, the electron collision frequency is on the order of 10^{11} to 10^{13} collisions per second. Therefore, for rocket exhaust diagnostics at atmospheric pressure utilizing EM waves in the microwave band, the wave behavior is characterized as that in a collisional plasma. For such a case, the EM wave propagation trends are very complex, and therefore the data reduction equations do not afford simplification as they do when evaluating low-collision plasmas. An experimental program in this regime should use the nonsimplified equations as presented in this paper for the determination of electron density and collision frequency from attenuation measurements. The experimental results showed that attenuation measurements in a laboratory-scale rocket exhaust plume can successfully provide ranking of propellants according to their propensity to produce electrons.

Acknowledgments

The U.S. Army Missile Command (MICOM) Propulsion Directorate supported this research under Contract DAAH01-92-D-R006. The expertise of personnel at the University of Alabama in Huntsville Aerophysics Facility is gratefully acknowledged. MICOM solid-rocket test and measurement facility personnel are thanked for their help in performing the tests.

References

[1]Heald, M. A., and Wharton, C. B., *Plasma Diagnostics with Microwaves*, Wiley, New York, 1965; reprint, Krieger, Malabar, FL, 1978.

[2]Hutchinson, I. H., *Principles of Plasma Diagnostics*, Cambridge Univ., Press, New York, 1987.

[3]Balwanz, W. W., "Rocket Exhausts and Their Interactions with Electromagnetic Waves," in *AGARDOGRAPH '87, Fluid Dynamics Aspects of Space Flight*, Vol. 2, AGARD, 1966, pp. 307–330.

[4]Gordon, S., and McBride, B. J., "Computer Program for Calculation of Complex Chemical Equilibrium Compositions, Rocket Performance, Incident and Reflected Shocks, and Chapman–Jouget Detonations," NASA SP-273, 1971.

[5]Coleman, H. W., and Steele, W. G., *Experimentation and Uncertainty Analysis for Engineers*, Wiley, New York, 1989.

[6]Blevins, J. A., Frederick, R. A., and Coleman, H. W., "An Assessment of Microwave Measurement Techniques in Rocket Exhaust Applications," AIAA Paper 94-0671, Jan. 1994.

T. C. Lin
Associate Editor

Gravity Anchoring for Passive Spacecraft Damping

Renjith R. Kumar*
Analytical Mechanics Associates, Inc.,
Hampton, Virginia 23666

Introduction

MAGNETIC dampers have been used by several gravity-gradient stable spacecraft to provide passive damping. These require no power or communication capability to perform the function of nulling postinjection or deployment rates and to maintain stable steady-state oscillations. Magnetic dampers have been used for passive attitude control in several spacecraft,[1] including the Geodetic Earth Observing Satellite, the Geodynamics Experimental Ocean Satellite, the Gravity Gradient Test Satellite, the Timeation Satellite, and the Long Duration Exposure Facility (LDEF).

A magnetic damper consists of two concentric spheres. The inner sphere contains a permanent magnet that aligns with the Earth's magnetic field lines, and the outer sphere is attached to the spacecraft body. A viscous fluid (for the viscous damper) or a diamagnetic material (for the eddy-current damper) is used between the spheres to produce a damping torque whenever there is relative angular velocity between the two spheres. The damping torque must be large enough to resist relative angular motion, yet small enough to allow the inner magnetic core to maintain orientation with the geomagnetic field.

The major disadvantages of magnetic anchoring are as follows:

1) As the spacecraft orbits the Earth, the local orientation of the Earth's magnetic field changes continually with respect to the local vertical and local horizontal (LVLH). This causes the inner core attitude to vary with respect to the LVLH, which produces undesirable torques on the spacecraft trying to maintain an LVLH attitude. This is especially true for high-inclination orbits passing through the magnetic poles.

2) The damper provides only two-axis damping. Restoring torques exist that align the inner-magnet axis with the Earth's magnetic field lines, but no torque exists to restrict the inner magnet from rotating about the magnetic field vector. For example,[2] in near-equatorial orbits, damping about the pitch axis is small.

In this paper, the use of a new damping methodology, dubbed gravity anchoring, instead of the usual magnetic anchoring, isx proposed to alleviate the disadvantages incurred by the latter. Comparison between the two methodologies, including design considerations and combination of the two methods into a hybrid magnetic–gravity anchoring, is suggested.

Gravity Anchoring

The idea of gravity anchoring is simple. Why not use a gravity-gradient stable inner core instead of the magnet in the viscous or eddy-current damper discussed earlier? If sufficient gravity-gradient restoring torque and inertia can be provided to the inner core, then gravity anchoring could be realized. The natural frequencies[3] of the linearized gravity-gradient stable dynamics of the inner and outer core must be separated to prevent any phase lock between the inner and outer core, which in turn would prevent damping. An immediate advantage of using the gravity anchor is that this damper does not induce any undesirable steady-state perturbations, since the inner and outer core are both trying to align to the same gravity field. Even though gravity-gradient torques cannot be generated about nadir (yaw axis), gyroscopic coupling[4] could be utilized to provide restoring yaw torques. Thus the gravity anchoring yields three-axis damping. The only remaining question is "Can the inner core be designed to have sufficient inertia and gravity-gradient restoring stiffness?" The answer depends on the spacecraft inertia, size, allowable decay time constant, and pointing requirements. In the following section, the passive damping design problem is addressed, and a comparison between magnetic and gravity anchoring is performed.

Design Approach

Given an approximate spacecraft configuration, i.e., the inertia properties and the shape, the first task is to identify the maximum anticipated pitch bias angle. This bias angle may be due to biased disturbing solar or aerodynamic torques. Asymmetry and nonzero center-of-pressure–center-of-gravity (CP–CG) offsets can cause these biased disturbing torques. The next task is to determine the minimum required damping to prevent Garber[3] instability. This arises for all gravity-gradient spacecraft in the presence of a constant disturbance torque in the pitch axis. This condition is predicted by the linearized equations of motion when the linearization is performed about the biased pitch, roll, and yaw positions. The pitch bias produces instability in the roll–yaw channels. The pitch bias at which the spacecraft goes unstable is a function of the inertia properties and the damping.[5] Let K_G denote this minimum damping coefficient that avoids Garber instability.

The next task is to define an acceptable decay time from worst-case initial deployment attitude and attitude rates. A good guess can be obtained from simulation, assuming the inner core reference frame to always align with an LVLH frame, i.e., the inner core is perfectly anchored to LVLH. Let this minimum damping coefficient that satisfies the decay-time constraint be denoted by K_T. Then the minimum required damping coefficient is $K_D = \max[K_G, K_T]$.

Now the inner core has to be designed so that the restoring magnetic torque on the inner core (for magnetic field anchoring) or the restoring gravity-gradient torque on the inner core (for gravity field anchoring) is larger than the maximum anticipated damping torque. Moreover, the larger the inertia of the inner core, the smaller the effect of the damping torque on its attitude motion. This is particularly important if the restoring torques are small. For magnetic anchoring, large restoring torques can be achieved by increasing the strength of the magnet, which indirectly implies larger mass and size of the passive damper. The disadvantage is the larger steady-state perturbative torques and oscillations. For gravity anchoring, the same can be achieved by increasing the gravity-gradient restoring torques (difference of inertias of the inner core)[4] and the inertia of the inner core, which map directly into larger mass or size of the inner

Received Oct. 7, 1994; revision received March 20, 1995; accepted for publication March 21, 1995.

*Senior Engineer. Member AIAA.